Hybridization sensing by electrical enhancement with nanoparticles in nanogap

Chun-Chi Chen, Fu-Hsiang Ko,[a] and Edward Yi Chang[b]
Institute of Nanotechnology and Department of Material Science and Engineering, National Chiao Tung University, Hsinchu 300, Taiwan

Feng-Chih Chang
Department of Applied Chemistry, National Chiao Tung University, Hsinchu 300, Taiwan

Shiao-Wei Kuo
Department of Materials Science and Optoelectronics Engineering, National Sun Yat-Sen University, Hsinchu 804, Taiwan

(Received 17 June 2008; accepted 22 September 2008; published 1 December 2008)

In this work, the monolayer of gold nanoparticles within 72 nm gap has been proposed to function as a DNA sensor. The authors suggest that the nanoparticles in the nanogap could act as hopping sites which amplify the conductance of hybridized DNA strands. The conductance amplification between single strand and hybridized DNAs through gold nanoparticles is observed. Various concentrations of capture and target DNA are discussed for optimal hybridization sensing purpose. With the help of 1 nM capture DNAs, this sensor is able to analyze target DNA sequences at very low concentration of 1 fM. Furthermore, by means of adjusting the denature temperature to 60 °C, even single mismatch hybridization could be discriminated. © *2008 American Vacuum Society.*
[DOI: 10.1116/1.3002489]

I. INTRODUCTION

DNA is the most important molecule with genetic information in living species. The analysis of gene expression and the gene analysis of single nucleotide polymorphism (SNP) are regarded as the major application fields of DNA chip.[1]. Today most DNA analyses are performed with an optical technique. In this case, fluorescence light of an optical marker molecule attached to the DNA strands is detected. The instrumentation requires to utilize charge coupled device camera, optical filters, lenses, and laser light. Furthermore, the methods described so far, a major challenge in DNA assay is to avoid the utilization of analyst amplification such as polymerase chain reaction, so the selectivity and the sensitivity of DNA assay become key points to overcome above issue. However, a simpler readout principle can be realized by detection of an electrical current in a comparatively small setup. According to this, scientists have tried to analyze DNA through its electronic properties. Among these methods, biochemical assay systems based on the electrochemical detection concepts have reported in several studies.[2–4]. Other detection methods employing oligonucleotide-functionalized gold nanoparticles for colorimetric detection have been developed.[5,6]. Furthermore, some studies introduce nanoparticles for the enhancement of conductance difference[7–9] between single strand and hybridized double strands. Among these literatures, direct electronically sensing approach by various promising devices was always very attractive. However electrode gap-type sensing devices[9–11] required a further chemical enchantment step (silver ion or multilayer gold nanoparticles) to amplify conductance signal. In this study, monolayer gold nanoparticles were used to self-assemble into the nanogap devices to measure the conductance variation without further complicated chemical treatment. Various conditions of nanogap for concentration changes were demonstrated and analyzed. The effect of specific heating temperature on improving the sensing discrimination for the proposed device was also evaluated.

II. EXPERIMENTAL

All chemicals and solvents were reagent-grade quality and used without further purification unless otherwise noted.

A. Experimental procedure for DNA biochip assembly

The analytical concept based on sandwich assay and electrical detection is shown in Fig. 1. The electron shape–beam lithography was used to fabricate the gold-gap device. Prior to the assembly of thiol-contain capture DNA strand with gold nanoparticles, gold nanoparticle monolayer was immobilized onto the device surface. Then, target DNA strands with both fully complementary and single mismatch were applied to hybridize, individually. In order to distinguish the assemble force between fully complementary and single mismatch hybridizations, the denaturing treatment by 60 °C water was applied. The sequences of the oligonucleotides used in this study are illustrated in Fig. 2.

The use of gold nanoparticles was to amplify the electrical current through nanogap. The gold nanoparticles cannot only provide a binding site for thiol-containing capture DNA strands but also a hopping center for electrons when applying

[a]Electronic mail: fhko@mail.nctu.edu.tw
[b]Electronic mail: edc@mail.nctu.edu.tw

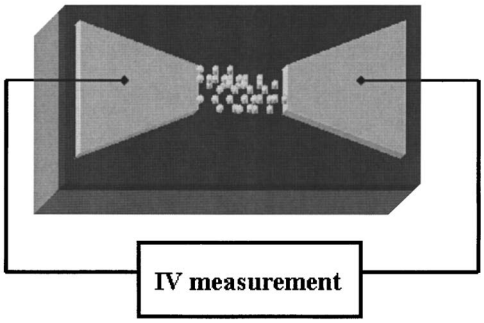

FIG. 1. Schematic of the proposed nanoparticle-based DNA sensor.

external voltage. The concentration level of DNA molecules in nanogap electrodes was varied from the low to high concentration of target DNA.

B. Synthesis of gold nanoparticles and fabrication of nanogap electrode device

Dispersed gold nanoparticles were prepared in aqueous solution by using a chemical reduction method. The synthetic procedure for the 10 nm gold nanoparticles was similar with the published paper.[12] Briefly, 1 mM $HAuCl_4$ (100 ml) was heated near its boiling point under the vigorous magnetic stir, and then 35 mM sodium citrate solution (10 ml) was added. The resulting solution was maintained at a reflux condition for 30 min. The color of the solution changed from yellow to brownish red upon the chemical reduction of $HAuCl_4$ mediated by citrate; this color change indicated the successful synthesis of the gold nanoparticles. A scanning electron microscopy SEM image indicated that the gold nanoparticles we had synthesized was spherically shaped, and we estimated that the average particle diameter is near 10 nm.

The fabrication of nanogap structures was depicted in Fig. 3. A silicon wafer was grown with a thickness of 500 nm silicon dioxide film by plasma-enhanced chemical vapor deposition. Then, the 400-nm-thick resist was spin coated onto the silicon dioxide and the electrodes with sub-100 nm gaps were patterned by electron beam lithography (Leica Weprint model 200 stepper, Jena, Germany). Prior to the deposition of the 60 nm gold film, a 5 nm titanium film was sputtered onto the surface to ensure the better adhesion. Finally, acetone solvent was used to lift-off the resist.

Capture DNA (5'thiol-Modifier)

3 ' - CCT AAT AAC AAT TTA TAA CTA TTC CTA - 5 '

Complementary Target DNA

5 ' - GGA TTA TTG TTA AAT ATT GAT AAG GAT - 3 '

Single Mismatch Target DNA

5' - GGA TTA TTG TTA AAT ATT TAT AAG GAT - 3'

FIG. 2. The DNA sequences for the capture, target, and single mismatch oligonucleotides.

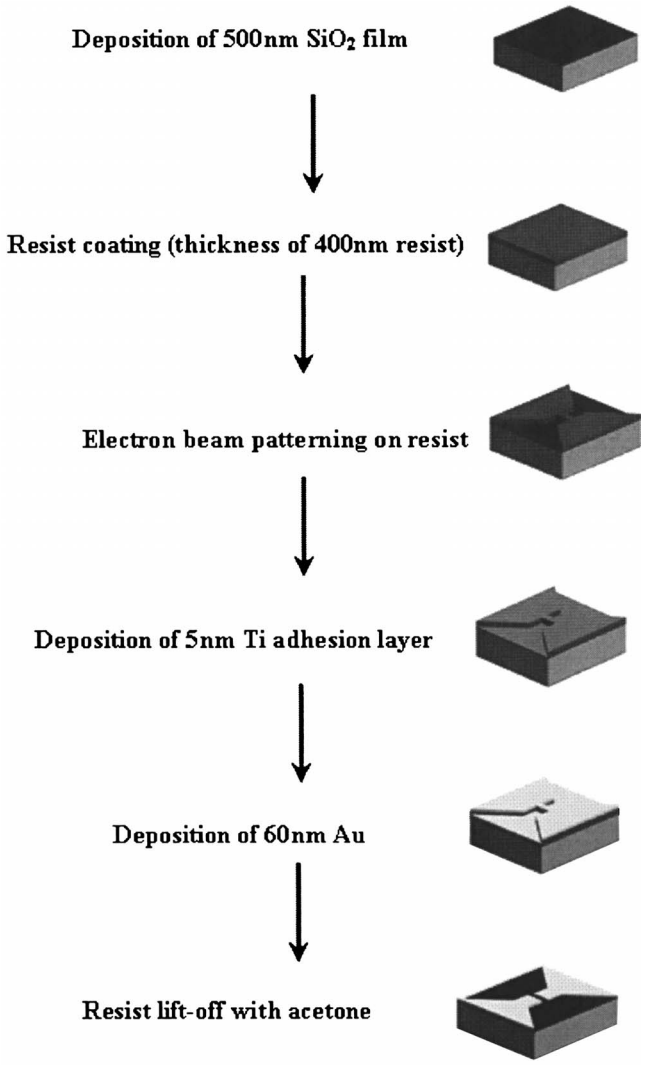

FIG. 3. Detailed fabrication processes for the gold nanogap electrode on silicon dioxide film.

C. Self-assembly of gold nanoparticles onto the silicon dioxide surface

The linker molecule between silicon dioxide film and gold nanoparticles within the gap of the drain and source electrodes was 3-mercaptopropyltrimethoxysilane (MPTMS). At first, the linker was dissolved in 10 ml of dimethyl sulfoxide (DMSO) to reach 5 mM concentration. Prior to immersing the nanogap structures into the linker solution, the solution was heated to 100 °C. The wafer was removed, carefully rinsed with DMSO, and blown dry with N_2. The wafer was then immersed into the gold nanoparticles solution and reacted for 1 h for the monolayered self-assembly. The nanoparticles/MPTMS/SiO_2 sandwich structures were stabi-

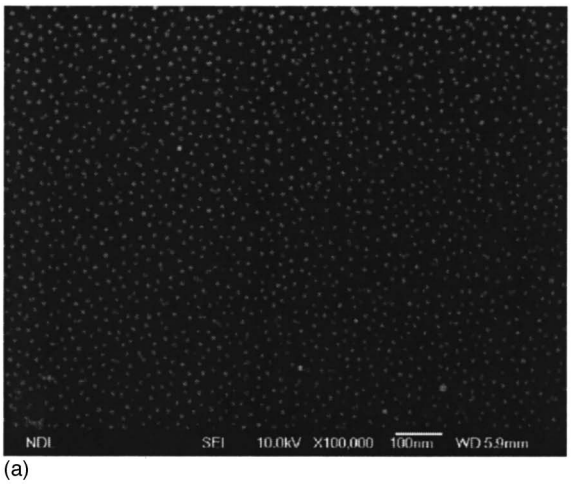

(a)

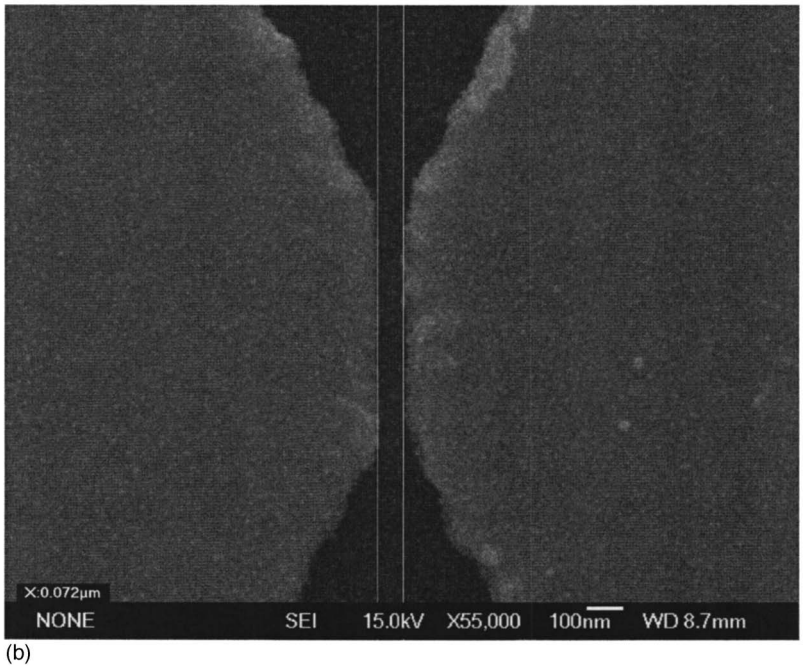

(b)

FIG. 4. High-resolution scanning electron microscopic images of (a) a self-assembled monolayer of 10 nm gold nanoparticles on the silicon dioxide film and (b) a self-assembled monolayer of 10 nm gold nanoparticles in the nanogap.

lized through specific $Au-NH_2$ interactions.[13] Figure 4(a) shows the gold nanoparticle morphology on a SiO_2/Si substrate by high-resolution scanning electron microscopy (HR-SEM). The 10 nm gold nanoparticles have previously assembled onto the sensor by the procedures mentioned above. Figure 4(b) illustrates that the 10 nm gold nanoparticles are assembled into the 72 nm gap.

D. DNA hybridization and denature

The sequences of the capture, target, and mismatch oligonucleotides (cDNA, tDNA, and mDNA, respectively) are illustrated in Fig. 2. The tDNA molecule is complementary to the cDNA. In comparison with the tDNA sequence, the mDNA contains only one mismatch base pair. A 10 mM 4-(2-hydroxyethyl)-1-piperazineethanesulfonic acid (HEPES) (J.T. Baker Chem. Co.) solution was prepared. Buffer (5 mM ethylenediaminetetraacetic acid) was used to adjust the HEPES to *p*H 6.6. The 27-mer cDNA (with three concentration levels, i.e., 1 nM, 1 pM, and 1 fM) was deaerated in HEPES buffer. The self-assembled gold-particle monolayer was immersed in the cDNA solution for 1 h under room temperature, followed by rinsing with *p*H 6.5 sodium phosphate buffer containing sodium chloride (SPSC) buffer (i.e., 50 mM sodium phosphate and 0.3*M* NaCl) to remove noncovalently bonded DNA, and was dried under N_2. The substrates were immersed in tDNA and mDNA solutions for 2 h to hybridize, followed by immersing in a SPSC buffer to remove excess reagents. The resulting chip was washed with 0.3*M* phosphate buffered saline buffer to ensure the tDNA and mDNA hybridization. The chips were then immersed in de-ionized water for 2–3 s and dried with N_2 purge.

After treatment, these samples were put in a desiccator under vacuum for drying and preservation. Then, the measurable *I-V* curves of the array biochip were obtained from a HP 4156A precision semiconductor parameter analyzer in the voltage ranges from −1 to +2 V with a scan rate of 1 mV/s. The denature process was to wash result chip (hybridized) by

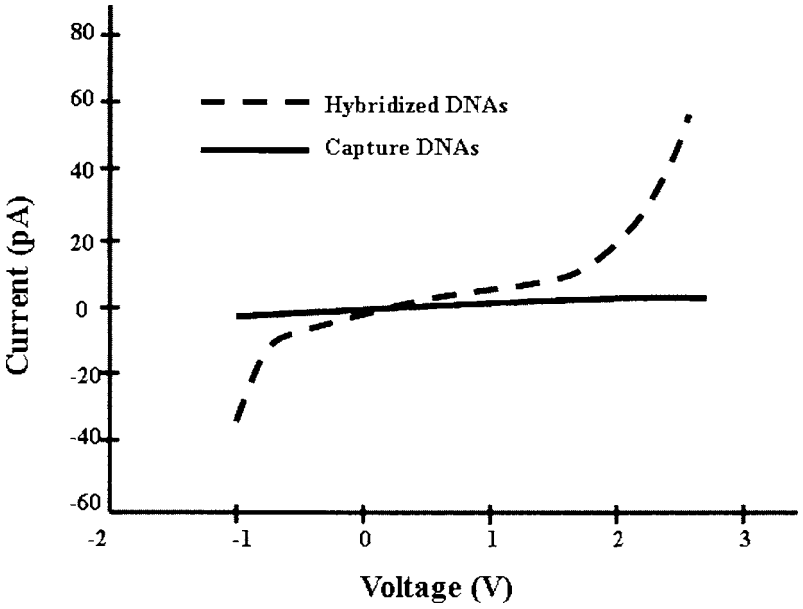

FIG. 5. Current-voltage characteristic of single- and double-stranded DNA sensor (assembly by 10 nm gold nanoparticles) in the nanogap. The recording rate is 1 mV/s.

de-ionized water at different temperatures. Then, *I-V* measurement was taken again. Fully complementary hybridized double strand DNAs will be denatured at certain temperature, which is higher than single mismatch one.

III. RESULTS AND DISCUSSION

Prior to optimize the suitable concentrations of capture and target DNA, the electrical property for 1 nM capture and hybridized target DNA was evaluated. In Fig. 5, the current-voltage curve of single stranded capture DNA was flat. This observation indicated the electrons did not pass through the single stranded DNA tethering with gold nanoparticles. In contrast, the current-voltage curve of double strand hybridized DNA exhibits the nonlinear electrical characteristics, i.e., pseudo-Ohm's behavior. The result of conductance enhancement through gold nanoparticles verified the effect of electron tunneling from DNA molecule and was attributed to the diffusive thermal hopping. Electrons and holes were indeed able to shuttle along a single DNA molecule over a distance of a few nanometers.[14–16] The diffusive thermal hopping process was related to (1) electron tunneling through AT base pair inside DNAs and (2) thermal activated electron hoping which occurred between or inside DNAs. The overall phenomenon of those two mechanisms was similar as diffusion motion. Since the tunneling process only happen along AT pair inside the DNA itself,[14–16] the thermal hopping becomes dominate over long range electron transport. In our case, additional gold nanoparticles would act as hopping site for thermal activate hopping points; therefore, the diffusive current would increase owing to reduced hopping distance. The nonlinear electrical characteristics might be attributed to electrons passing through the heterojunction which existed energy barrier between DNA itself and gold nanoparticles. In order to discriminate the single and double stranded DNAs, all the measured conductances were operated at applied voltage of 2 V.

In order to observe the electrical characteristic of hybridization, the nanogap devices with monolayered gold nanoparticles were assembled on various concentrations of capture DNAs, and then applied different concentrations of target DNAs to hybridize. The conductance for various concentrations was shown in Fig. 6, and all the conductance data were observed at applied voltage of 2 V. Interestingly, the sample from the higher capture DNA concentration exhibited higher conductance. In addition, with the 1 nM target DNA concentration, the conductances were 4×10^{-12}, 2×10^{-12}, and 0.8×10^{-12} S for 1 nM, 1 pM, and 1 fM capture DNAs, respectively. The reason for the playing role of DNA molecule was explained in the following. The DNA was a charged molecule. Charge transfer via stacked aromatic bases (π-π stacking) for DNA had been proposed.[17,18] Hybridized double-stranded DNA owned more compact π-π stacking which contributed to electron delocalization. Gold

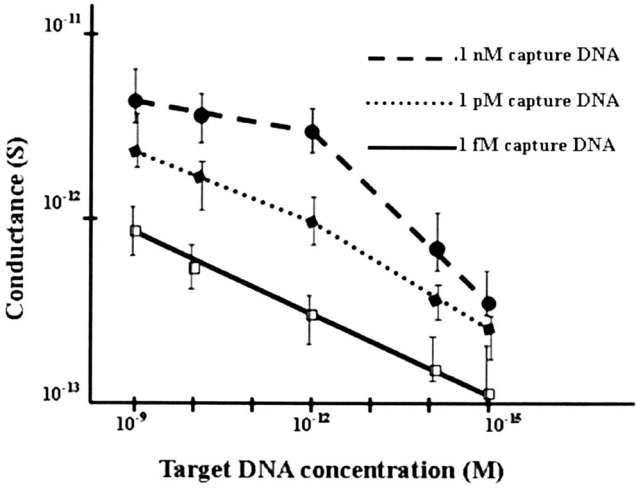

FIG. 6. The relationship of conductance with respective to various target DNA concentrations for various concentration levels of capture DNA.

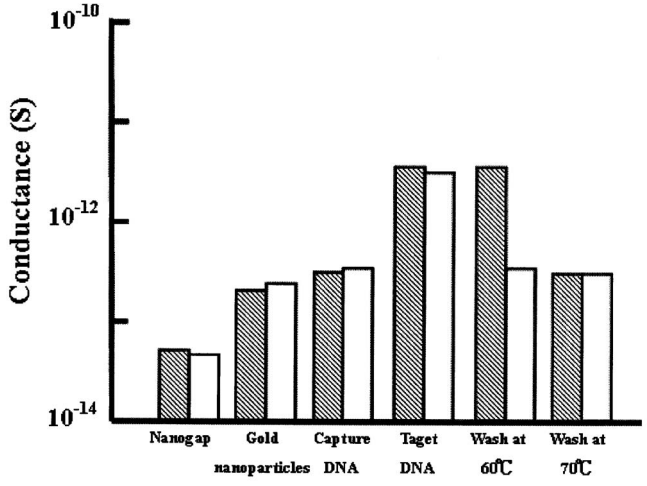

FIG. 7. The obtained conductance under various assembling conditions for complementary DNA (gray region) and mismatch DNA (white region) samples.

nanoparticles provided an extra hopping site in the gap, and therefore, amplified the conductance for double-stranded DNA.[19] The higher capture DNA concentration led to more binding on gold nanoparticles, therefore, more target DNAs could be attached for hybridization. However, with higher capture DNA concentrations, for example, 1 nM, the conductance of hybridized DNAs tended to saturate with increasing target DNA concentrations in Fig. 6. In contrast, the 1 pM and 1 fM capture DNA samples exhibited the linear conductance relationship with target DNA concentrations. The reason of saturation of high capture DNA concentration was attributed to the limitation of binding sites of gold nanoparticles.

The limit of detection for DNA molecule in Fig. 6 is in the femtomolar range and demonstrates the better analytical detection limit than the nanowire-based, mass spectroscopic and piezoelectric sensors.[20–22] Hybridization discriminated ability can be described as the conductance deviation between capture DNA and hybridization DNA. The 1 fM capture DNA was applied on the nanogap, and the measured conductance was 0.1×10^{-12} S. However, the conductance of hybridization DNAs with 1 fM target DNA was also 0.1×10^{-12} S. This observation suggests that the case of 1 fM capture DNA hybridized with 1 fM target DNA fails to discriminate single-stranded and hybridized double-stranded DNAs. In contrast, the conductance of hybridization sample with 1 nM capture and 1 fM target DNAs still had 3.2-fold higher than single stranded capture DNA. This result indicated that the capability of this sensor was operated under 1 nM capture DNA by 1 fM target DNA hybridization detection.

The effectiveness of DNA sensor was evaluated not only on the detection of small sample volume but also to the capability of discriminating the single base pair mix match through temperature treatment.[7] In Fig. 7, the conductance of the fully complementary DNA and single mismatch samples for each experimental step was shown. Prior to hot water washing, the conductance signals for both samples are almost the same. However, after 60 °C water treatment, conductance of mismatch hybridized DNA decreased. This confirmed that only single-strand DNA existed on the sensor surface. In contrast, fully complementary sample remained the same conductance. Furthermore, the water washing at 70 °C removed the second stranded DNA. The conductance signal from the sensor demonstrated only capture DNA on the surface. Hence, single base pair mismatch target DNA can be discriminated through the 60 °C water treatment.[7] This finding suggested the potential application of the developed biosensor to the field of SNP identification in the future.

IV. CONCLUSIONS

In this study, a DNA sensor for SNP identification through temperature treatment is successfully developed. The sensor uses the gold nanoparticles within nanogap to amply the electrical signal. The limit of detection for the DNA biochip is near 1 fM, which provides a sensitive and label-free diagnosis biosensor for future rapid disease detection. In addition, single mismatch hybridization can be discriminated by means of adjusting the denature temperature to 60 °C.

ACKNOWLEDGMENTS

The authors wish to thank the National Science Council of Taiwan for financially supporting this research through Contract Nos. NSC 96-2120-M-009-009 and NSC 95-2113-M-009-032-MY3.

[1]J. J. McCarthy and R. Hilfiker, Nat. Biotechnol. **18**, 505 (2000).
[2]E. M. Boon, D. M. Ceres, T. G. Drummond, M. G. Hill, and J. K. Barton, Nat. Biotechnol. **18**, 1096 (2000).
[3]T. G. Drummond, M. G. Hill, and J. K. Barton, Nat. Biotechnol. **21**, 1192 (2003).
[4]T. J. Huang, M. H. Liu, L. D. Knight, W. W. Grody, J. F. Miller, and C. M. Ho, Nucleic Acids Res. **30**, e55 (2002).
[5]R. Elghanian, J. J. Storhoff, R. C. Mucic, R. L. Letsinger, and C. A. Mirkin, Science **277**, 1078 (1997).
[6]T. A. Taton, C. A. Mirkin, and R. L. Letsinger, Science **289**, 1757 (2000).
[7]J. Fritz *et al.*, Science **288**, 316 (2000).
[8]Y. Weizmann, F. Patolsky, O. Lioubashevski, and I. Willner, J. Am. Chem. Soc. **126**, 1073 (2004).
[9]S. J. Park, T. A. Taton, and C. A. Mirkin, Science **295**, 1503 (2002).
[10]C.-C. Chen, C.-Y. Tsai, F.-H. Ko, C.-C. Pun, H.-L. Chen, and P.-H. Chen, Jpn. J. Appl. Phys., Part 1 **43**, 3843 (2004).
[11]C.-Y. Tsai, T.-L. Chang, C.-C. Chen, F.-H. Ko, and P.-H. Chen, Microelectron. Eng. **78**, 546 (2005).
[12]M. A. Hayat, *Colloidal Gold-Principles, Methods and Applications* (Academic, San Diego, 1989) Vols. 1 and 2.
[13]F. K. Liu, Y. C. Chang, F. H. Ko, T. C. Chu, and B. T. Dai, Microelectron. Eng. **67**, 702 (2003).
[14]Y. G. Yang, P. G. Yin, X. Q. Lia, and Y. J. Yan, Appl. Phys. Lett. **86**, 203901 (2005).
[15]B. Giese, J. Amaudrut, A. K. Köhler, M. Spormann, and S. Wessely, Nature (London) **412**, 318 (2001).
[16]M. Bixon, B. Giese, S. Wessely, T. Langenacher, M. E. Michel-Beyerle, and J. Jortner, Proc. Natl. Acad. Sci. U.S.A. **96**, 11713 (1999).
[17]D. B. Hall, R. E. Holmlin, and J. K. Barton, Nature (London) **382**, 731 (1996).
[18]M. R. Arkin, E. D. A. Stemp, R. E. Holmlin, J. K. Barton, A. Hormann,

E. J. C. Olson, and P. F. Barbara, Science **273**, 475 (1996).
[19]C.-C. Chen *et al.*, Appl. Phys. Lett. **91**, 253103 (2007).
[20]F.-H. Ko, Z.-H. Yeh, C.-C. Chen, and T.-F. Liu, J. Vac. Sci. Technol. B **23**, 3000 (2005).
[21]S. Taylor, R. F. Tindall, and R. R. A. Syms, J. Vac. Sci. Technol. B **19**, 557 (2001).
[22]F.-H. Ko, Y.-C. Hsu, M.-T. Wang, and G.-w. Huang, Microelectron. Eng. **84**, 1300 (2007).